

Simulating kink instabilities of solar magnetic fluxropes

Z. Mei^{1,2}, R. Keppens^{1,3}

¹ *Centre for mathematical Plasma Astrophysics, Department of Mathematics, KU Leuven, Celestijnenlaan 200 B, B-3001 Leuven, Belgium*

² *Yunnan Observatories, Chinese Academy of Sciences, P.O. Box 110, Kunming, Yunnan 650011, PR China*

³ *School of Astronomy and Space Science, Nanjing University, Nanjing 210093, PR China*

Introduction

Research on twisted magnetic flux ropes (MFRs) are of critical importance to interpret many eruptive phenomena on the Sun. Helical MFRs are implied by many observations and core of corresponding theoretical models^[1] for eruptive processes. Higher twist of the field lines generally means more free magnetic energy, hence more flares can be produced, which can be more energetic.

Due to the motivation from observations, magnetohydrodynamics (MHD) kink modes in cylindrical line-tied loop^[2, 3] and T&D model^[4] have been studied intensively. Galsgaard & Nordlund^[5] investigated kink instabilities under different magnetic configurations, and distinguish two processes, external kink and internal kink. Kink instabilities in nonlinear regime, studied by numerical simulations^[2, 3], involve an intense current concentration that develops along the whole flux rope, and magnetic reconnection may occur in the vicinity of these current layers. Torok, Kliem & Titov^[6] and Kliem & Torok^[7] have studied kink instabilities of T&D model to highlight the curvature effect, and found that the growth of long-wavelength ($m = 1$) mode is slowed down by ambient magnetic field eventually although twists are higher than typical criterial value 3.5π . Torok & Kliem^[1] furthermore produced a confined eruptive filament with helical feature, which is highly consistent with the observations.

In this work, we perform a study of the kink instabilities of T&D model for different twist numbers and more realistic solar atmosphere by performing two isothermal 3D MHD simulations. Internal dynamical processes of MFRs as a consequence of kink instabilities have been investigated in detail.

Numerical models and Schemes

As shown in upper panel of Figure 1, magnetic field of T&D model is constructed by a force-free circular MFR with the total current I and a background field from combination of a pair of magnetic charges and a line current buried d under the photosphere $z = 0$. Un-

der the assumption of thin MFR ($a \ll R$), equilibrium of MFR can decompose into internal and external ones. Here, a is minor radius of MFR and R is major radius. The external equilibrium of MFR has been realised by magnetic field from magnetic charges. The outward self-force due to the curvature of MFR has been balanced by confinement force from magnetic charges. The internal equilibrium of MFR is due to mutual balance between toroidal and poloidal component of magnetic field, which comes from poloidal and toroidal current of MFR respectively. Except the achievement of equilibrium, a line current have been used to decrease the twisted turns of MFR to observational value in the solar corona, typically less than 4π .

In the lower panel of Figure 1, twisted turns^[4] of MFR upon the photosphere is

$$\text{turns}(r) = 2 N_t(r) \arccos \frac{d}{R} \quad (1)$$

where r is the distance from the toroidal axis of MFR and $N_t(r)$ can be expressed as

$$N_t(r) = \frac{R B_{\text{polo}}(r)}{r B_{\text{toro}}(r)}, \quad (2)$$

where B_{polo} and B_{toro} are poloidal and toroidal components of magnetic field (for more detail, refer to [4]). At the surface of MFR $r = a$, it approximately equals to $(R^2 I)/(a^2 I_0)$. In addition, safety factor $q(r)$ of MFR is just a inverse of $N_t(r)$, which has been widely used to study instabilities in Tokamaks.

Initial conditions of this study consist of uniform density distribution (equals to 1), magnetic field of T&D model (average strength inside MFR ≈ 2) and $\beta \approx 0.01$. Two configurations of T&D model, low twist and high twist cases, have been used (see also case 1 and 5 shown in Table 1 of Torok, Kliem & Titov^[6]), in which I_0 equal to -23.8 and total current I inside MFR equal to 1.03 and 7.68 respectively. The boundary condition in the bottom of simulation box is line-tied, and other five boundaries are open.

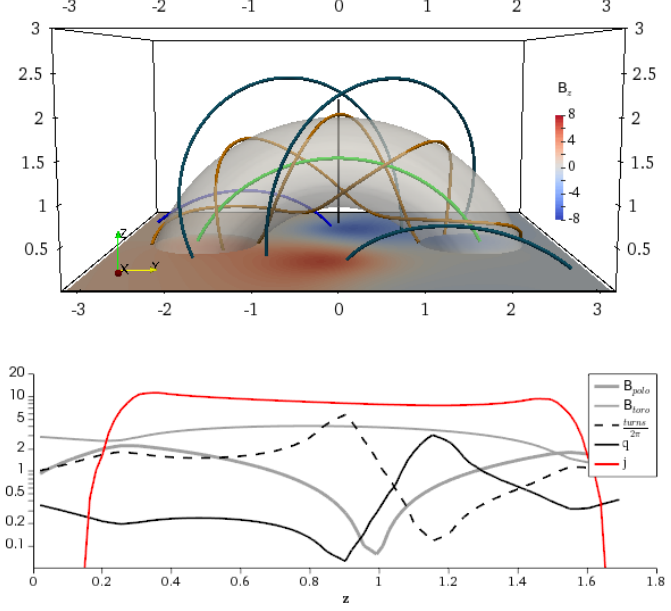


Figure 1: (Top) Initial magnetic configuration (3D colour curves) for averaged $\text{turns} = 2.1\pi$, distribution of normal magnetic field (shadings) on the panel $z = 0$, and translucent isosurface marked the surface of MFR. (Bottom) Distributions of toroidal and poloidal magnetic field components, turns and safe factor along the cutting from $z = 0.6$ to 1.2 on the central axis shown in the top panel.

All physical quantities in simulation are dimensionless with units $5 \times 10^9 \text{ cm}$, $1.28 \times 10^7 \text{ cm s}^{-1}$, $3.89 \times 10^2 \text{ s}$, $1.67 \times 10^{-14} \text{ g cm}^{-3}$, 2.76 Pa , 5.89 G and $2.95 \times 10^{11} \text{ A}$ for length, velocity, time, density, pressure, magnetic field and line current respectively. The computational domain is a 3D uniform box of sizes $-4 < x < 4$, $-4 < y < 4$, and $0 < z < 8$ in Cartesian coordinate, and resolve evolution of MFR with 200^3 .

The governing isothermal MHD equations are solved by MPI-AMRVAC^[8] code. Numerical schemes are a third-order accurate, shock-capturing fine volume spatial discretization, combining an HLL Riemann solver and a third-order flux reconstruction, with a three-step Runge-Kutta time marching. The divergence free of magnetic field is controlled by a diffusive approach, which diffuses away any numerically divergence.

Internal kink instabilities

Benefiting from realistic fine-beta atmosphere and higher calculation resolution to resolve dynamical processes inside the MFR, more details of internal current structure have been resolved (As shown in Figure 2), which did not get enough attention in previous works. These works studied external kink instabilities

based on T&D model with two end point of MFR fixed to the photosphere. The development of external kink highly depend on the ambient magnetic structure out of MFR^[1, 7], and not be effected by the internal structure of MFR. In contrast, internal kink mode is sensitive to the current profile $j(r)$ inside the MFR and leads to an internal magnetic field untwisting internal to the resonant layer.

Figure 2 show evolution snapshots of current distribution at different times for the weakly twisted MFR and fine-beta atmosphere ($turns \approx 2.1\pi$ and $\beta = 0.01$), in which internal kink instability has been spotted. Because safety factor inside the MFR varies from larger than 1 nearby the axis of flux rope to below

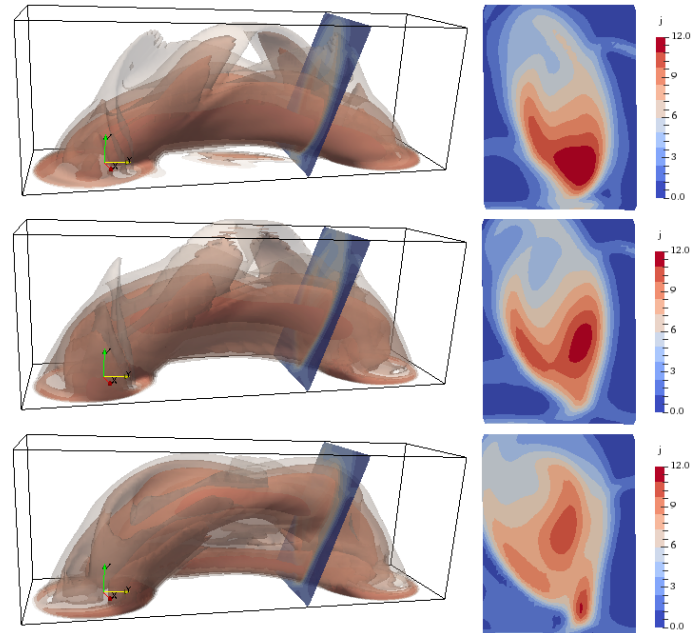


Figure 2: (Left) Snapshots of the current distribution at three time instances ($t = 8.4, 10.2$ and 12). Colors on the slice and isosurface represent different values of current. (Right) Current distribution on the slices, which are the same slices shown in Left panels.

0.2 on the surface of MFR, the MFR is unstable to internal kink mode, and interior current structure begin to redistribute along the toroidal axis of MFR after the launching of this simulation, and evolve from a almost uniform distribution on poloidal cross section of MFR into two-component structures at $t = 8.4$. At this time, equivalent minor radius of each components decrease dramatically, while major radius R keep unchanged and magnetic strength does not change too much. One component become unstable to external kink mode^[1] , because of Kruskal-Shafranov condition. However, this external mode has almost confined inside of MFR, which obscure the difference nature between two different kink modes.

In the meanwhile, external kink mode also grows in another component but slowly, i.e. arouses slight upward movement, which compete with line-tied effect. The line-tied effect tend to avoid the upward motion of MFR. In the end, part of MFR remain in its place, which leads to a appearance of third fine current structure (can be seen from the snapshot at $t = 12$), and separate from MFR inevitably, as an independent current sheet under the MFR. It is important to note that formation of this current sheet is significantly different from already exist model for flare/CME phenomena, such as flux rope model, in which a current sheet under the flux rope forms from converge of external magnetic field during upward movement of flux rope.

As for the highly twisted cases ($turns \approx 4.9\pi$), MFRs first experience a external kink instability process. Then MFRs break up into two parts, each of which experience almost the same process occurred in the weakly twisted MFRs. Furthermore, the interaction between two parts lead to more complex shape of whole magnetic structures.

In conclusion, the internal kink instabilities can even occur inside low twisted MFR, which is initial stable to external kink instability. The resultant dynamical process inside MFR changes its internal current distribution violently, and lead to the formation of finer current sheets inside and around the MFR. These finer structures can be of relevance to magnetic reconnection and particle acceleration mechanism, and so provide a sets of eruptive phenomena.

References

- [1] Török, T., & Kliem, B. 2005, ApJL, 630, L97
- [2] Velli, M., Lionello, R., & Einaudi, G. 1997, SoPh, 172, 257
- [3] Baty, H. 2000, A&A, 353, 1074
- [4] Titov, V. S., & Démoulin, P. 1999, A&A, 351, 707
- [5] Galsgaard, K., & Nordlund, Å. 1997, JGR, 102, 219
- [6] Török, T., Kliem, B., & Titov, V. S. 2004, A&A, 413, L27
- [7] Kliem, B., & Török, T. 2006, PhRvL, 96, 255002
- [8] Keppens, R., Meliani, Z., van Marle, A. J., et al. 2012, JCoPh, 231, 718